

MULTIVARIATE POPULATION BALANCES VIA MOMENT AND
MONTE CARLO SIMULATION METHODS

Daniel E. Rosner, Robert McGraw, and Pushkar Tandon

June 2003

By acceptance of this article, the publisher and/or recipient acknowledges the U.S. Government's right to retain a nonexclusive, royalty-free license in and to any copyright covering this paper.

Research by BNL investigators was performed under the auspices of the U.S. Department of Energy under Contract No. DE-AC02-98CH10886.

Multivariate Population Balances via Moment and Monte Carlo Simulation Methods: An Important Sol Reaction Engineering Bivariate Example and “Mixed” Moments for the Estimation of Deposition, Scavenging, and Optical Properties for Populations of Nonspherical Suspended Particles

Daniel E. Rosner,^{*,†} Robert McGraw,[‡] and Pushkar Tandon^{†,§}

Department of Chemical Engineering, High-Temperature Chemical Reaction Engineering Lab, Yale University, New Haven, Connecticut 06520-8286, and Environmental Sciences Department, Brookhaven National Laboratory, Upton, Long Island, New York 11973-5000

Reactors or crystallizers synthesizing valuable particles can be formally described by combining the laws of continuum transport theory with a population balance equation governing evolution of the “dispersed” (suspended) particle population. Early examples necessarily focused on highly idealized device configurations and populations described locally using only *one* particle state variable, i.e., “size” (length or volume). However, in almost every application of current/future importance, a *multivariate* description is required, for which the existing literature offers little guidance. We describe here our recent research on an instructive *bivariate* prototype of physical interest (coagulating, sintering nanoparticles of prescribed composition, etc.) that will, hopefully, motivate a broader attack on important *multivariate* population balance problems, including those describing continuous molecular mixtures. We illustrate the use of both physically based bivariate “mixed” moment and Monte Carlo simulation methods amenable to future generalization. Multivariate extensions, improved and fully coupled rate laws, and consideration of interacting (coexisting) populations will be required to deal with future sol reaction engineering problems using similar strategies/techniques.

1. Introduction and Objectives

Particle production from *vapor* precursors must be accurately predicted and controlled, motivating considerable theoretical and experimental research.^{1–4} Rarely is the particle *size* alone sufficient to characterize the “state” of a particle because particle properties of greatest current interest cannot generally be related only to size (say, *volume*, *v*, or a volume-equivalent diameter). Moreover, the additional state variables of interest (e.g., shape, crystallinity, chemical composition, etc.) usually evolve dynamically in response to simultaneous rate processes and changing environmental conditions. Because a goal of sol reaction engineering (SRE) is to predict the conditions necessary to efficiently produce particles of desired size, shape, crystallinity, and composition (“stoichiometry”), etc., efficient simulation methods capable of dealing with *multiple-particle state variables* are now urgently needed.

While our emphasis has been on submicron particle synthesis from the *vapor* phase, especially using combustion techniques, the above-mentioned comments (on the need for a multivariate approach) apply equally well to the design/optimization of industrial crystallizers⁵ (in which particle populations evolve in supersaturated, usually turbulent, *liquids*), as well as particle precipitation from *supercritical fluids* (SCFs).⁶

Under these circumstances, it is surprising how sparse the literature is when it comes to the formulation/treatment of multivariate population balance situations. For this reason, we have decided to call attention here to a fruitful recent prototype *bivariate* population balance problem of physical importance on which considerable progress *has* recently been made. Thus, we will deliberately restrict ourselves to an instructive limiting case in which the chemical composition and crystallinity are fixed but the aerosol *size* and *shape* distributions respond to simultaneous Brownian coagulation and finite-rate “spheroidization”.⁷ These are, of course, the circumstances deliberately studied in our recently reported steady laminar counterflow diffusion flame experiments on alumina nanoaggregates^{8–10} using both laser light scattering (LLS) and thermophoretic sampling (TPS) techniques. A systematic comparison of such well-defined measurements with simulations, a program initiated in refs 11 and 12, can also be used to extract physicochemical parameters (e.g., the effective activation energy for surface diffusion on “nanoparticles”) that may be new or relatively inaccessible by more conventional “routes”. Not surprisingly, multivariate populations of suspended nanoparticles also occur in rather different applications, including “continuous mixtures” of *macromolecules* (see, e.g., section 8). In all of these applications, including those involving hydro-sols or particles suspended in SCFs, we anticipate the utility of the moment-based and Monte Carlo (MC) based simulation methods briefly described below (sec-

* To whom correspondence should be addressed. E-mail: daniel.rosner@yale.edu

† Yale University.

‡ Brookhaven National Laboratory.

§ Present address: Corning Inc., Corning, NY 14831.

tion 5) and the physical/statistical relevance of certain “mixed” moments of the underlying jpdfs (see section 3).

Another important example of the need for more than one variable to represent the state of a suspended particle is found in the recent atmospheric chemistry literature targeting the climate effects of black carbon (BC). BC-containing aerosols cause local atmospheric heating (via solar energy absorption), and this, in turn, can cause changes in weather patterns through increased local convection, precipitation, and surface cooling. Moreover, through tropospheric transport of the warmed air, such climate changes can exert an influence even beyond the transport range of the aerosol itself.^{13,14} Here the aerosol “mixing state” is important, with model-based predictions¹⁵ indicating that *sulfate-coated BC particles*, formed by mixing, approximately double the contribution of BC to global warming, relative to models that treat the BC-aerosol as “unmixed”. This more general mixing state is treated within the framework of a 1D (“univariate”) “sectional” model (section 5) by allowing for the presence of multiple size distributions and defining several probability density functions (pdfs) consisting of sulfate and BC in coated and uncoated forms which subsequently interact through coagulation. The comparative efficiency of the bi- and multivariate “moment methods” that we will emphasize below should allow these to be viable and computationally advantageous alternatives to multidistribution sectional models for representing “generally mixed” particle populations in atmospheric models.

2. A Bivariate Description of Particle Populations: $n(v, a, x, t)$

Our prototype bivariate model, currently undergoing further development, is that first proposed by Koch and Friedlander.⁷ Here, particle *volume* and surface *area* were selected as the two independent particle state variables, and these authors deliberately studied the simplest uncoupled rate laws governing Brownian coagulation and area change, with the latter rate assumed to be “surface-energy driven”, i.e., proportional to the instantaneous difference $a - a_{\min}(v)$, where $a_{\min}(v)$ is the area of a *sphere* of volume v (see eq 2 and section 7). Rather than assuming that particle morphology does not influence the collision frequency of particles of known volume, as an interim measure one can introduce the *fractal dimension*, D_f , as a *prespecified* morphological parameter (see, e.g., refs 16–18). However, more generally, fractal dimension will be a *distributed* parameter (cf. electron micrographs included in refs 8 and 9), not known a priori.

Returning to this v, a level of particle description, if $n(v, a, x, t)$ is the local (position x), instantaneous (time t) *number density distribution function*, then its mixed moments, $M_{k,l}$, are defined by the $\int \int v^k a^l n(v, a) dv da$ over all positive values of v and a . Here, the exponents k and l need not be positive, integers, or equal, and the corresponding *dimensionless* moments, $\mu_{k,l}$, are defined by $M_{k,l}/(\bar{v}^k \bar{a}^l N_p)$, where $N_p = M_{0,0}$ is the *total* particle number density (irrespective of the particle volume or area), $\bar{v} = M_{1,0}/M_{0,0}$ is the number-mean (average) particle *volume*, and $\bar{a} = M_{0,1}/M_{0,0}$ is the number-mean particle *surface area*. Some of these mixed $M_{k,l}$ values, and their *dimensionless* counterparts, $\mu_{k,l}$, are of special physical interest, as will be described/illustrated below. We should also note that self-consistency of our mathematical model requires that the particle *volume frac-*

tion, $\phi = M_{1,0} = \bar{v}N_p$, be “small”,²⁰ but not so small as to render the Brownian coagulation rate negligible. In our flame experiments,^{8–10} ϕ was, at most, on the order of 10^{-6} (i.e., 1 ppm).

In general, the evolution equation satisfied by the local, instantaneous number density distribution function $n(v, a, x, t)$ is a nonlinear integro-partial differential equation (IPDE), containing *partial derivatives* with respect to the independent variables a , x , and t , as well as (in the case of particle–particle interactions) *integrals* over the particle volume and area variables (see, e.g., ref 4 or 17). For the present discussion, we will restrict ourselves to the special case of (a) no explicit²¹ dependence on the space coordinate(s), x , (b) Brownian coagulation (a “two-body” process), (c) particle area reduction due only to surface-energy driven sintering, (d) negligible particle volume changes due to vapor condensation, and (e) negligible nucleation or particle breakup. Then the population balance equation (PBE) formally simplifies to the IPDE:

$$\partial n / \partial t = (\partial n / \partial t)_{\text{coag}} - (\partial / \partial a) [\dot{a} n] \quad (1)$$

where the “coalescence” (last) term may be regarded as (minus) the “divergence” of the flux $\dot{a} n$ in the a space, and the symbolic coagulation term appearing on the right-hand side (RHS) may be explicitly written (in the continuous Smoluchowski form) as the instantaneous difference between two double integrals, the first of which has the integrand $(1/2)\beta(v, v-v', a-a') n(v', a', t) n(v-v', a-a', t) dv' da'$ with the upper integration limits v, a . Here, of course, we must supply the coagulation rate “constant” β , as well as the rate law governing the coefficient function $\dot{a}(v, a, \dots)$ in the coalescence (area reduction) term.^{7,22} In all of the work described here, as already mentioned, this latter function has been chosen to be of the “relaxation” form

$$-\dot{a} = [a - a_{\min}(v)] / t_f(v, a, \dots) \quad (2)$$

where the indicated characteristic *fusion* time function is mechanism- and environment-dependent (see, e.g., refs 7, 16, 22, and 23). In the present cases, once these functions are specified, we wish to track the evolution of $n(v, a, t)$ using eq 1, from its (prescribed) initial condition $n(v, a, 0)$. Often, this initial condition is simply taken to be a “monodispersed” population of spheres of common (“primary”) volume v_1 and corresponding area $a_1 = a_{\min}(v_1) = 4\pi(3v_1/4\pi)^{2/3}$. For a critical discussion of the various assumptions that have been made in evaluating the relevant collision rate constant, $\beta(v, v-v', a', a-a')$, the reader is referred to the above-mentioned references, as well as ref 24.

It should also be remarked that, for MC simulations, in effect one attacks the IPDE(1) directly, obtaining successive numerical “realizations” of $n(v, a, t)$. However, in the case of moment methods, the differential equations satisfied by the chosen dependent variables $M_{k,l}$ are obtained from eq 1 by integration over all v, a , after premultiplying the IPDE(1) by $v^k a^l$. In implementing the method of moments (MOM), we seek to avoid any method that requires that we *presume* the functional form of $n(v, a, t)$.

While this particular bivariate mathematical model is admittedly highly idealized, we discovered that much can be learned from its adoption by pursuing its practical consequences. Not only do we expect that our strategies and mathematical techniques will be ap-

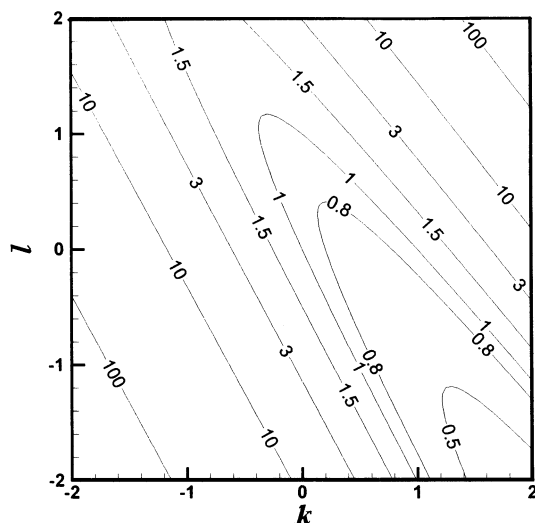


Figure 1. Typical dimensionless moment surface (for uncoupled rate laws) for free-molecule coagulation and sintering in the long-time limit: $D_f = 1.8$, $\text{Dam}_f = 10^{-2}$ (using the nine moment method of Wright et al.²⁶). Note that, because the particular moments $\mu_{1,0}$, $\mu_{0,1}$, and $\mu_{0,0}$ are necessarily unity (see footnote, Table 1), the "peninsula-shaped" contour $\mu = 1$ passes through the three separated points (1, 0), (0, 1), and (0, 0) on the (k, l) plane. For the parametric dependency of $\mu_{1,-2/3}$ (on Dam_f and D_f in the free-molecule limit), see Figure 3.

plicable to other multivariate models, we will also show that the recently acquired body of results for the pdf(v, a) problem can be used to make rational estimates of many aerosol or hydrosol physical phenomena of current engineering importance,²⁵ including the way such suspended particle populations will scavenge solutes, elastically scatter visible light, and deposit (by various mechanisms) onto surfaces from flowing fluids. All of these calculations will be seen to follow from appropriate simulations of the jpdf(v, a, x, t) satisfying the PBE, *without* presuming its functional form.

As is also discussed/displayed below and from generalization of previous univariate research (summarized in ref 4), in some applications the *bivariate* jpdf(v, a) has been shown to approach a "self-preserving" form, in the sense that $n(v, a, t) \cdot \bar{v}\bar{a}/N_p$ becomes a function of time only via the *two* independent dimensionless variables: v/\bar{v} and a/\bar{a} (for examples, see refs 16 and 17). Rather than calculating and displaying this particular "surface", for many applications we find that it is sufficient, and perhaps even more useful, to calculate/display the so-called "mixed moment surface" (or $\mu_{k,l}(k, l)$ defined above and displayed in Figure 1).

While the assumption of "approximate" or "local" bivariate self-preservation may even be possible in certain time-dependent environments of practical interest, our "seeded" counterflow diffusion flames⁸⁻¹⁰ (in which the particles experience local heating rates of ca. 40 000 K/s) are, notably, *not* among them, requiring a fully dynamical treatment.^{11,12} Nevertheless, the early availability of the above-mentioned MC-based self-preserving bivariate PSD results^{16,17} successfully guided the subsequent development of more economical yet acceptably accurate moment methods applicable in this multivariate, fully dynamical domain of SRE.^{12,22,26}

3. Physical Significance of Certain Mixed Moments²⁵

Extending our earlier univariate work on the total mass deposition rates of sols onto solid surfaces,²⁷⁻³⁰ we

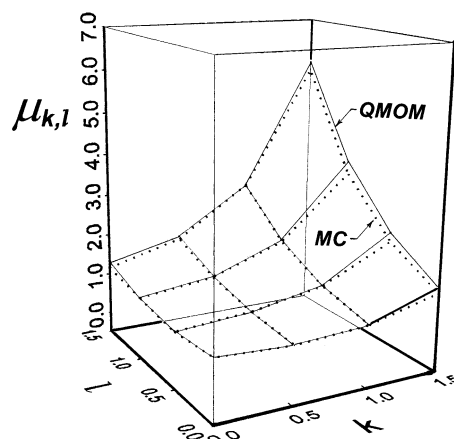


Figure 2. Comparison of MC- and QMOM-based dimensionless moment surfaces (for uncoupled rate laws) for continuum coagulation and surface-area-driven sintering in the long-time limit: $D_f = 1.8$, $\text{Dam}_f = 10^{-2}$ (after ref 26).

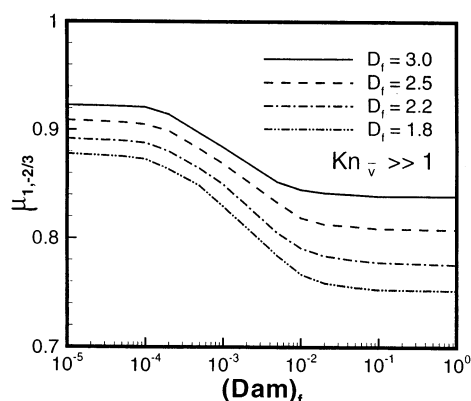


Figure 3. MC-based prediction of the dependence of the dimensionless mixed moment $\mu_{1,-2/3}$ (Table 1) on the Damkohler parameter Dam_f for free-molecule coagulation and simultaneous sintering (coalescence): self-similar (long-time) case with prespecified D_f values (indicated) (after ref 17). In practice, D_f and Dam_f will *not* be independent (see, e.g., ref 12), making the dependence of $\mu_{1,-2/3}$ on Dam_f weaker than shown here.

now find that certain dimensionless mixed moments of the mainstream particle population are physically significant in the present bivariate case. For a representative example, consider the particular *dimensionless* moment $\mu_{1,-2/3}$ [actually shown in Figure 3 vs the parameter Dam_f governing the relative *sintering* (fusion) rate, for the particular case $D_f = 1.8$]. This particular moment, with $k = 1$ and $l = -2/3$, can be regarded as a first approximation to the dimensionless deposition rate *ratio* R defined by

$$R = \frac{\text{actual total mass deposition rate from the prevailing aerosol population}}{\text{reference deposition rate (in the same environment) if all particles had volume } \bar{v} \text{ and area } \bar{a}} \quad (3)$$

for the case of isothermal *convective-diffusion mass transfer* in the (aerosol) limit of a very large Schmidt number, when the suspended particles are in the free-molecule regime ($Kn_p \gg 1$).¹⁷ This claim follows from the approximate dependencies: particle diffusivity of $D \sim a^{-1}$ and mass deposition rate $\sim vD^{2/3}n \, dv \, da$. Table 1 lists a number of additional dimensionless mixed moments of $n(v, a, \dots)$ of particular physicochemical interest. Note that such results can be derived for any "kernel"

Table 1. Selected Dimensionless Mixed Moments ($\mu_{k,l}$) of Physical Interest

moment index		Knudsen	
k	l	number	physical significance of $\mu_{k,l}$
0	1/2	$\ll 1$	vapor scavenging (diffusion-controlled) rate
0	1	$\gg 1$	vapor scavenging (diffusion-controlled) rate
-2/3	+1	all	allows \bar{a} and a''' to be found from evolution of \bar{v} and N_p
1	-1/3	$\ll 1$	$Sc \gg 1$ convective-diffusion deposition rate (mass or volume)
1	-2/3	$\gg 1$	$Sc \gg 1$ convective-diffusion deposition rate (mass or volume)
2	-1/2	$\ll 1$	gravitational sedimentation rate
2	-1	$\gg 1$	gravitational sedimentation rate
3	-1	$\ll 1$	eddy impaction
3	-2	$\gg 1$	eddy impaction

^a By the definitions of population-mean *volume*, mean *area*, and the dimensionless jpdf $\Psi = \bar{v} \bar{a} n(v,a)/N_p$, it follows that the particular moments $\mu_{1,0}$, $\mu_{0,1}$, and $\mu_{0,0}$ are identical to *unity*, a feature which can be used as a numerical accuracy check.

(or “weighting function”; here the mass deposition rate coefficient) expressible as a *power law* in the selected state variables (see appendix 1), irrespective of the nature (shape, etc.) of the underlying pdf.

Accurate values of certain mixed moments are also of special interest because, in an important class of approximate methods for solving population balance problems, one proceeds by deriving/solving a closed set of coupled differential equations governing the evolution of a preselected set (section 5) of dimensional “lower moments”, some of greater physical interest than the “reconstructed” pdf itself (see sections 4 and 5). Indeed, a Gaussian *quadrature*-based MOM (QMOM) developed by McGraw,³¹ and adopted for crystallizer modeling by Marchisio et al.,³² has recently been generalized to apply to bivariate populations of immediate interest here.²⁶ Indeed, using only nine moments, this bivariate QMOM predicted continuum regime mixed moments in acceptable agreement with the results of a MC-based numerical method (see section 5 and Figure 2). This QMOM approach promises to be particularly important in future SRE applications because the differential equations governing each mixed moment, $M_{k,l}$, are of the same form (“convective-diffusion-source”)³³ as those governing any reactive chemical *species* in the same flow. Because of this property, QMOM will facilitate articulation of the population balance approach with available, increasingly powerful computational fluid dynamics (CFD) simulation/design/optimization tools.

It can also be shown (appendix 2) that such mixed moment surfaces (e.g., such as that sketched in Figure 1) necessarily satisfy a “convexity” (concavity) condition that can be exploited in several ways, including the facilitation of moment *interpolation* and/or *extrapolation*.^{34–36} Perhaps less obvious, this property can also be used as a check on the numerical accuracy of moment evolution calculations. For example, nonlinear approximations used in advective transport algorithms can yield “nonphysical” moment sets that locally *fail* the convexity test. This can be a serious problem in atmospheric transport models where grid cell dimensions are often necessarily large (see, e.g., Wright et al.³⁷). Fortunately, this problem can be overcome by advecting moment sets as a vector quantity with elements (the normalized moments) that can be viewed as *internal coordinates* of the local pdf.³⁷

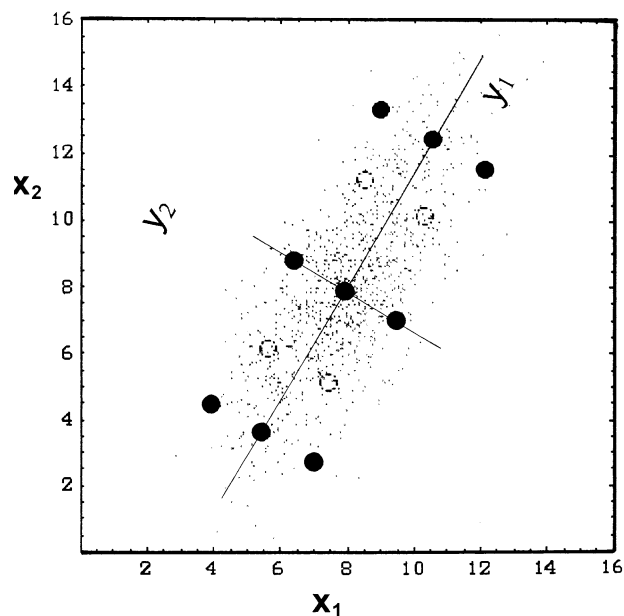


Figure 4. Assignment of quadrature points in the “principal coordinates” frame. The schematic shows 1000 points sampled from a bivariate pdf in the original state variables: x_1 and x_2 . The principal coordinates are y_1 and y_2 , respectively, as briefly discussed in section 3. Open circles: Q points derived from moments $\{0, 1, 2\}$ along each principal axis (these have equal weights). Closed circles: Q points derived from moments $\{0, 1, 2, 3, 4, 5\}$ along each principal axis (these have differing weights) (after ref 38).

Statistical Significance. Beyond their physical significance, the mixed moments are inherently statistical quantities that provide a convenient and especially useful set of parameters for characterizing statistical properties of the pdf. In very recent investigations, a standard tool from statistics, called *principal component analysis* (PCA), has been combined with quadrature concepts to obtain a general multivariate version of the QMOM.³⁸ Central to applying PCA is the generation of the *covariance matrix* (\mathbf{M}), the elements of which are mixed moments. For a bivariate problem $\mathbf{M}_{1,1} = M_{2,0} - M_{1,0}^2$, $\mathbf{M}_{2,2} = M_{0,2} - M_{0,1}^2$, $\mathbf{M}_{1,2} = M_{1,1} - M_{1,0}M_{0,1} = \mathbf{M}_{2,1}$. For a multivariate problem of dimensionality n , the covariance matrix is $n \times n$ and symmetric. The eigenvalues of \mathbf{M} are the principal components, or variances, along the principal axes defined by the corresponding eigenvectors. The moments entering \mathbf{M} are used, together with the normalization $M_{0,0}$, to generate quadrature abscissas (cf. Figure 4, showing a schematic of the population in the two state variables labeled x_1 and x_2) and weights that, in turn, are used to update the moments in a multivariate QMOM simulation. Details of the method will appear elsewhere.³⁸ There is no fundamental limit to the number of pdf variables that can be handled, and other important advantages are inherent in the combined PCA-QMOM method. For example, the largest eigenvalues and corresponding eigenvectors describe the coordinates of maximal variance in the principal frame and are the ones most important for characterizing statistical properties of the pdf. As an added bonus, when the dimensionality n is large, selecting the subset of largest eigenvalues and corresponding eigenvectors of \mathbf{M} can result in dimensional reduction of the full dynamics by projecting out the most significant coordinates—as in other data/image applications for which PCA-based “compression” is often used.

4. Dimensionless Mixed Moments as “Surrogates” for Local pdf(v, a, x, t) and pdf “Shape Factors”

Clearly, a finite subset, $\mu_{k,l}$, of dimensionless mixed moments “parameterizes” the joint normalized $\Psi = \text{fct}(\eta_1, \eta_2, t/t_{\text{coag}}, \dots)$ (where, say, $\eta_1 \equiv v/\bar{v}$ and $\eta_2 \equiv a/\bar{a}$) and constitutes an alternative description to the more obvious one of providing, say, an array of Ψ_{ij} values (“discrete ordinates”). Indeed, in the implementation of the QMOM (section 5), an efficient numerical means for “constructing” the pdf associated with a subset of mixed moments is, in fact (implicitly), provided. Rather accurate evolution of a bivariate $n(v, a; \mathbf{x}, t)$ has been accomplished using a 36-moment method, but most of the moments of physical interest could be adequately predicted by using a nine-moment description (see refs 12 and 26). For those quantities of interest (e.g., experimental “observables”) that *cannot* be simply expressed in terms of a small number of particular mixed moments (section 7), Gaussian quadrature techniques can be used, provided the required weighting function is not too “spiky”.³⁹ From another viewpoint, the $\mu_{k,l}$ values can be regarded as *dimensionless shape factors* characterizing, say, the underlying pdf($\eta_1, \eta_2, t/t_{\text{coag}}; \text{Dam}_f, D_f$). Indeed, they arise in a natural way when one interrelates various types of “means” for the same physical quantity.¹⁷ Depending on the experimental technique used (with its intrinsic weighting factors), some means are inevitably more relevant than others, revealing a sensitivity to the *shape* of the underlying multivariate pdf.

5. PBE Modeling Issues: Computation of pdf($v/\bar{v}, a/\bar{a}, t/t_{\text{coag}}; \text{Dam}_f, D_f$) and Its Mixed Moments

Before turning to a brief description of PBE computational methods, we first raise/address two broad questions of immediate concern if we are to develop successful SRE multivariate mathematical models:

Q1. What *is* a “promising” choice of particle state variables?

Q2. In MOM-based multivariate PBE computations, which moments should we track?

We take these sequentially.

5.1. “Promising” Choices of State Variables?

Considering the variety of partially sintered alumina “aggregate” shapes/morphologies that have shown up on our TEM-grid images (using the technique called TPS),^{8–10,40} one might prematurely conclude that a description of the particle population based only on the particle state variables: *volume* v and “wetted” surface *area* a , has little chance of succeeding! However, in part because Brownian coagulation is intrinsically “volume-preserving” (see, e.g., Friedlander⁴) and the area-equivalent diameter $(a/\pi)^{1/2}$ plays such an important role in transport theory^{33,41,42} in both Knudsen number limits, and also because systematic corrections due to “nonsphericity” {conveniently quantified here by the dimensionless sintering “driving force”: $\xi \equiv [a/a_{\min}(v)] - 1$ } can be introduced, it is remarkable how far one *can* go with only these *two* state variables (see, e.g., Rosner and Pyykonen,¹² who, in fact, used v and the *difference* (or “excess” area) $a - a_{\min}(v)$ in implementing BV-QMOM when $Kn \gg 1$).

More generally, the choice of state variables will be dictated by such considerations as (C1) the level of description needed to predict those engineering quanti-

ties of immediate interest, including those quantities accessible to direct measurement (e.g., LLS signal, aggregate projected area, chemical composition, crystallinity, etc.), (C2) “orthogonality” or “independence” of the state variables chosen,^{38,43} and (C3) availability of relevant experimental data or theoretical results required for the rate laws that appear in the PBE and govern evolution of the corresponding mixed moments. Of course, in any new situation such a choice will never be “unique”, and even matters of individual “taste” cannot (should not!) be excluded. Indeed, as new experimental methods, faster computational speeds, and new/more powerful theoretical methods/results become available, it is likely that what appeared to be an optimal choice of particle state variables in the past becomes amenable to further improvement.

5.2. How Many and Which Moments Should Be Tracked?

In any practical case, an equally important decision must be made as to the particular subset of moments to use as the basic jpdf surrogates (dependent variables in the convective-diffusion equations representing the jpdf evolution) for the problem at hand. Recent BV-QMOM examples [in terms of v and a (or excess area): $a - a_{\min}(v)$] used either 9 moments, or 36 moments, depending on the “fidelity” of the jpdf representation required.^{12,26} A 36-moment representation of the local, instantaneous jpdf(v, a) used $M_{k,l}$ with $k, l = 0, 1/3, 2/3, 3/3, 4/3$, and $5/3$, allowing for sufficiently accurate Gaussian numerical quadratures for the case of the continuum Brownian coagulation kernel. This particular choice did *not* imply that each of the tracked moments was of particular physical relevance (cf. Table 1). Indeed, on the basis of physical relevance alone, the values of the *area* index, l , might have been integral powers of $a^{1/2}$ (not $a^{1/3}$). Rather, the chosen set simply “spanned” the region of mixed moment space of greatest physical interest *for the problem at hand*, without giving undo importance to “tails” of the jpdf. This “region of interest” definitely depends on the sol population properties being measured, or the phenomena of practical interest. A well-known example in the univariate,⁴⁴ spherical particle case deals with the consequences of measuring/displaying the alternate pdfs: $n(v, \dots)$, $v^{2/3}n(v, \dots)$, $vn(v, \dots)$, or, say, $v^2n(v, \dots)$. The first of these often betrays the existence of numerous nanoparticles of rather small volume, whereas the last of these dictates the elastic light scattering power of the suspended population, in the single-scattering Rayleigh limit. The two intermediate choices are relevant, respectively, to vapor (molecular solute) scavenging/growth, and, say, the volumetric extinction/emission of radiation. Therefore, depending on what sol properties are of interest/being measured, one might deliberately modify (select) the moments to be tracked. Of course, if a trivariate description must be invoked, one may be obliged to limit the number of mixed moments to a number not much greater than, say, 27 (or, perhaps, in simpler problems, 64), thereby limiting the number of quadrature points in each of the state variables chosen. These inevitable “tradeoffs”, some of which are presently under investigation, will probably have to be evaluated on a case-by-case basis. General guidelines are certainly needed and will facilitate future SRE modeling efforts.³⁸

5.3.1. MC-Based Methods. One of the earliest applications of the so-called MC method to coalescing dispersed-phase systems was demonstrated by Spielman and Levenspiel.⁴⁶ They studied the influence of

coalescence on the progress of chemical reactions occurring in the dispersed phase in a backmixed reactor, where the reactant concentration in the dispersed phase was again described by a nonlinear integrodifferential equation. Even for their spatially homogeneous system involving a monodisperse population, a constant coalescence rate, and a single internal variable, Spielman and Levenspiel⁴⁶ realized/emphasized the efficacy of the MC method because analytical solutions were simply not possible and alternative numerical methods cumbersome. Although the precise mathematical connection between the method and the PBE was established later,^{47,48} this early work helped motivate the development of MC methods for a wider variety of particle technologies. These include simulations of the local coagulation rate term, $(\partial n/\partial t)_{\text{coag}}$, in the particle population balance IPDE (see, e.g., refs 16, 17, 50, and 51). This can be done regardless of the complexity of the expression for the collision frequency (see section 2), although the algorithm may become costly to implement numerically. For population balances in which particle *volume* is the only relevant state variable, the MC method, while easy to program and implement, probably has no special numerical advantage over so-called sectional (essentially finite-difference) methods. However, as the required number of particle state variables increases, MC-based methods become computationally more attractive.^{16,52} In the present paper we are exploiting two state variable precedents,^{16,17,26} and we report/use mixed moments obtained from simulations of the population balance for an aerosol coagulating due to Brownian motion, simultaneously undergoing finite-rate coalescence (spheroidization). By examining the moments computed in this class of model problems, we gain a valuable understanding of many important features of the jpdf of particle volume and surface area for such populations, including their response to a Damkohler-like dimensionless parameter (constructed from the ratio of the characteristic *coagulation time* to the characteristic *sintering time*). For applying MC in more general 3D, transient environments, the method would be very similar to present applications of the so-called direct simulation (DS) MC method⁵³ to 3D rarefied *gas* flows. Here the underlying IPDE is the Boltzmann equation, where the integral ("collision") term is simulated by MC ("stochastically"), while the other terms are treated "deterministically".

More generally, it may be said that stochastic (MC-based) methods provide powerful tools for solving multivariate population balance problems, precisely where more conventional numerical methods, like sectional methods, become awkward to program and computationally prohibitive. While the versatility of MC methods has already been demonstrated for several bivariate problems,^{16,17,54–56} they are particularly attractive for PB problems requiring three or more internal variables.⁵² The theoretical basis for the application of MC methods to such population balance problems has been established by a number of authors.^{48,57,58} In effect, MC methods make use of probabilistic tools to predict the expected behavior of a population. A subset of the population is considered, and it is allowed to evolve in time under the influence of different physical mechanisms (aggregation, etc.) with transition probabilities (or frequencies) proportional to the kinetic rates of those mechanisms. The population evolution is determined by randomly choosing events from all possible transitions

based on the appropriate probabilities. Each event is separated from the subsequent event by a time interval, commonly referred to as the interval of quiescence,⁴⁷ which corresponds to the time between two collision events. It is estimated on the basis of the intrinsic system kinetics and helps establish the precise relationship between the real time and a MC step. The distinct events along with their corresponding intervals of quiescence are determined from the weighted probability distributions of all possible transitions. Pdf's determined from the behavior of this subset of the population are then used to estimate the quantities of interest for the entire population.

A number of advances in MC methodology make MC attractive for simulating the behavior of multi variate populations in many "quasi-Lagrangian" systems²¹ of practical interest. Smith and Matsoukas⁵⁰ and Lin et al.⁵⁹ have developed/applied the so-called "constant number" MC method, which allows for simulating aggregating populations even at long elapsed times. Eibeck and Wagner⁶⁰ have introduced the concept of "majorant kernel" to improve the efficiency of MC methods. Majorant kernels are chosen such that their simplified functional forms not only allow for efficient estimation of normalized transition probabilities but also significantly increase the fraction of "accepted events" during the simulation. Goodson and Kraft⁶¹ have improved on this method by developing majorant kernels with the same degree of homogeneity as the coagulation kernel itself. Majorant kernel methods are likely to be of particular interest for multivariate populations for which the coagulation kernels are complex functions of the various state variables.

It should be mentioned that stochastic methods provide solutions to the so-called "Master" equation, which includes probabilistic information of the system based on the individual particle behavior. The usual PBE is obtained by averaging the Master equation.⁴⁸ Thus, while the numerical solutions of the PBE give the average (expected) behavior of the population, MC solutions can also provide information about *fluctuations around the mean*, often important for very small populations (e.g., the postgelation phase of a gelling system). Indeed, stochastic methods have been shown to model such systems more accurately than the PBE approach.^{56,62}

5.3.2. QMOM-Based Simulation Methods. Presently available PBE simulation methods [especially those based on the so-called sectional (finite-difference) representations of the particle population balance] required to track the evolution of coagulating, restructuring populations, even in simple flow environments, are cumbersome, often requiring hours of CPU time on large work stations. However, our recent research²⁶ has led us to a potentially more efficient class of simulation methods for problems of current interest, also yielding dimensionless mixed moments in agreement with those predicted by the above-mentioned MC method. Instead of a "brute force" sectionalization in each variable (here v , a , etc.), which can become unwieldy even for bivariate problems, we have implemented a bivariate population-balance method using a generalization of the recent Gaussian QMOM approach.^{26,31} This simulation strategy, which provides a closed set of equations for the moments (in terms of the quadrature abscissas and weights), is currently being applied to the above-mentioned data sets, both using presently available rate

laws (for coagulation frequency, thermophoresis, and sintering)¹² in terms of the state variables, v and a , as well as rational improvements currently under development (see refs 24 and 63 and section 7). Quadrature-based moment simulation methods should prove useful not only for efficient laminar or turbulent aerosol and hydrosol³² reactor design/optimization/scale-up but also for practical *parameter estimation*, e.g., inferring the “best-fit” activation energy for alumina nanoparticle sintering by surface diffusion.²³

A noteworthy feature of the quadrature variant of MOM is that the positions of the quadrature points (the “abscissas”), and their “weights”, are *not* predetermined. Rather, following Gauss, these are optimally determined from the pdf moments themselves, resulting in a “closed” system of coupled equations. This has several advantages over choosing, for example, a set of equispaced abscissa values, or even (for a fixed interval) using the “precalculated” Gauss–Legendre abscissa values. First, one avoids having to predetermine the best spacing and range of the fixed abscissa set, which will most likely be time-dependent. Second, there is the issue of economy: one can uniquely describe six moments using just three abscissas and three weights if these are NOT predetermined. On the other hand, predetermining the abscissas doubles that number to six abscissas and six weights, and one might be left with an ill-conditioned inversion problem to compute the six weights! Indeed, upon carrying out such an inversion, one might encounter negative weights, a nonphysical situation that would play havoc in the rate laws governing subsequent population evolution.

While not central to our present emphasis, it should be mentioned that moment methods have the advantageous property that they can be applied directly to “discrete” as well as to “continuous” distributions (see, e.g., refs 35, 36, and 64), which is necessary in dealing with nanoparticles made up of only a small number of “monomer” (molecular) units. All that is required is that the relevant integrals be replaced by sums. Thus, one can calculate the moments of a discrete distribution of molecular clusters down to the monomer size and “evolve” these in accord with specified rate laws. Similarly, the MOM has been applied to the formation of discrete aggregates consisting of monodisperse primary particles and rates of aggregation described by a modified Smoluchowski equation.⁶⁴

5.3.3. Comments on Alternative PBE Simulation Techniques. For perspective, several remarks on alternative numerical simulation strategies may be useful here.

Perhaps the most obvious starting point is the so-called sectional approach, in which each state variable is discretized (see, e.g., ref 65 for the univariate implementation). Indeed, this basic method has been implemented^{19,26,65} for the prototypical bivariate model (including Brownian coagulation) emphasized here. However, even in the absence of state-dependent Brownian diffusion in physical space and for only two state variables, the programming and computational times are unattractive (the calculations shown⁶⁶ were carried out on a supercomputer). It should be mentioned that modifications of the univariate sectional approach have recently been proposed/used to model more general multivariate states of aerosol particle populations (see refs 67–70). Jeong and Choi⁶⁷ retain a 1D sectional model but employ two pdf's, one for volume [$vn(v)$] and one

for area [$an(v)$], defined on the same volume (v) coordinate. Separate dynamical laws are used to evolve the $vn(v)$ and $an(v)$ distributions. This model is analogous to a recent sectional treatment of internally mixed particles in the atmosphere.⁶⁹ In an internal mixture, particles of the same mass (or volume) have the same composition, whereas in the Jeong and Choi representation,⁶⁷ particles of the same volume section have the same surface area. Computation times were reported⁶⁷ to be reduced to $1/1000$ of that needed for the corresponding 2D sectional model. Yet, the number concentration, surface area equivalent diameter, and primary particle size and number were in good agreement with those obtained from the 2D full sectional model.

A so-called “modal” technique has been proposed/implemented as an alternative approach to modeling the population balance in complex flows. In this technique,^{71,72} it is assumed that the sol may be divided into several distinct but additive populations, called “modes”, each described by analytic distributions (usually log normals) that evolve almost independently. Like the moment method (MOM described above), the modal approach is computationally efficient, with far fewer variables to track than in the case of sectional (finite-element-type) methods. Recently, the modal approach has been extended to the modeling of multicomponent aerosols.⁷² The treatments, however, are based on modifications of a *univariate* approach, in which the modal composition is either set constant or considered to be dependent on the particle size. While this is an advance in the application of modal methods, such approximations do not permit, for example, the representation of generally mixed aerosols having two (or more) components; i.e., they are restricted to externally mixed or internally mixed particle populations for which a *univariate* pdf can be constructed.

For a recent review of several other numerical methods which have been used to attack population balance problems (mostly univariate), the reader is referred to ref 51.

6. Observables Not Expressible in Terms of Mixed Moments Alone

While some of the quantities measured/reported in Xing et al.^{8–10} are simple⁷³ moments of $n(v,a,...)$ (e.g., the local *particle volume fraction*, $\phi = M_{1,0}$), others are *not*, such as the optically inferred *rms gyration radius* and effective *fractal dimension* of the aggregate population.¹⁰ However, as long as one can assign⁷⁴ a meaningful *effective gyration radius* and *fractal dimension* to (an ensemble of) individual particles with volume v and area a , then the QMOM formalism allows such population-averaged quantities to be calculated (via Gaussian quadratures) however complex (nonpower law) these relationships may be.¹²

7. Current/Future Developments: Effects of Improved Rate Laws

Improved and more fully coupled methods for predicting both the *collision frequencies* of nonspherical particles and their mechanism-dependent *sintering rates* (via viscous flow? volume diffusion? surface diffusion?) have been under development^{22–24,63,75} and will be the subject of future papers.⁶³ Significantly, despite their more complex functional forms (i.e., not readily expressible as finite sums of powers of the chosen state variables), it is straightforward to incorporate these improved rate laws in the above-mentioned MC or

QMOM formalisms. However, bear in mind that their inclusion will not only modify the numerical values of all of the $\mu_{k,i}$'s but will also demonstrate that the actual ratios of physical interest (e.g., eq 1) are only approximately identifiable with the indicated $\mu_{k,i}$ values (Table 1). The magnitude of these "corrections" remains to be determined on a case-by-case basis. Preliminary results for the systematic *increase* in the higher moments of the self-preserving ASD due to the use of more rigorous MC-derived correlations for FA-FA' collision frequencies, and their consequences for the interpretation of elastic light scattering and the prediction of inertial deposition/impact breakup have recently been presented.^{24,63} Perhaps not surprisingly, the altered collision kernel also leads to a rather different moment evolution,⁶³ in some cases even to a nonmonotonic approach to the (shifted) asymptotic (self-preserving) values.

8. Implications for Nonequilibrium "Continuous Mixture Theory" (CMT)

While our present emphasis is on suspensions of bona fide particles, in some sense a complex mixture of hundreds, if not thousands, of nonspherical, heavy hydrocarbon *vapor* molecular species in a background gas (e.g., He and/or N₂) can be considered a population of "suspended nanoparticles". This viewpoint implies that the concepts/methods illustrated above apply equally well to such multivariate *vapor* populations. It is true that most previous applications of the so-called CMT have been confined to the case of a *single* state variable (usually *molecular weight*, m ; see, e.g., refs 76–81). However, in future applications of CMT, this univariate assumption will have to be relaxed, together with the ubiquitous (but not necessary) assumption of a *presumed* MWD functional form. The methods highlighted in this paper will clearly permit implementation of these important extensions of CMT.

8.1. Multivariate CMT Illustration. To briefly illustrate this analogy, consider a "dilute" mixture of a large number of molecular species in a background gas, each species of which is described, say, by the following state variables: m , σ , ϵ , δ , α , and ω , the acentric factor (often viewed as a surrogate⁸² for Z_c), where σ and ϵ are respectively the Lennard-Jones size and energy-well parameters, δ is the permanent dipole moment, and α is the polarizability. Suppose the local, instantaneous number density in this "hyperspace" is $n(m, \sigma, \epsilon, \delta, \alpha, \omega; \mathbf{x}, t)$, where m , σ , ϵ , δ , α , and ω are considered continuous variables. In general, these state variables will be "uncorrelated", i.e., truly "independent" variables; however, in certain special cases sometimes of practical interest (especially when all of the species are members of a "homologous" family of compounds, e.g., straight-chain alkanes), one may be able to uniquely relate each of the remaining state variables to m , i.e., $\sigma(m)$, $\epsilon(m)$, $\delta(m)$, $\alpha(m)$, $\omega(m)$, etc. In the more general case, certain mixed moments of the above-mentioned multivariate distribution function, n , may be of considerable physical relevance (see below), whereas the existence of a "tight" correlation between these state variables (as in the alkane example illustrated below) may allow a univariate description to be sufficient, i.e., involving only moments of $n(\dots, \mathbf{x}, t)$ with respect to molecular mass, m , alone.

8.2. Reduction to the Trivariate CMT Case. To fix ideas, consider the simple limiting case of a population of "large", "heavy" molecules adequately described

by the three state variables⁸² m , σ , and ϵ alone (e.g., imagine that $\delta = 0$ and α and ω are not *explicitly*⁸³ needed) suspended in a large excess of, say, N₂(g). Suppose, further, that one was interested in the diffusion-controlled mass rate of partial condensation of these molecules on a "cold" surface exposed to, or containing, this mixture. In the absence of an appreciable Ludwig–Soret contribution,⁸⁴ this rate will often³³ be proportional to the triple integral

$$\dot{m}''(\mathbf{x}, t) \sim \int \int \int m D_{\text{eff}}^{2/3} n(m, \sigma, \epsilon, \mathbf{x}, t) dm d\sigma d\epsilon \quad (4)$$

where $D_{\text{eff}}[m, \sigma, \epsilon, T(\mathbf{x}, t)]$ is the pseudo-binary Fick diffusion coefficient through the prevailing background gas, given, say, by Chapman–Enskog theory,³³ and the integral is carried out over all positive values of m , σ , and ϵ . Then, because the Chapman–Enskog collision integrals can usually be approximated as a power law (say, -0.17 exponent) in the relevant dimensionless temperature $T(\epsilon_{\text{eff}}/k_B)$, where $\epsilon_{\text{eff}} \approx (\epsilon \epsilon_{\text{N}_2})^{1/2}$, one finds that total local mass deposition rate, $\dot{m}''(\mathbf{x}, t)$, will be approximately proportional to a particular mixed moment: $M_{i,j,k}$ of $n(m, \sigma, \epsilon; \mathbf{x}, t)$ with respect to m , σ , and ϵ , where $i = 1$, $j = -4/3$, and $k = -0.057$. (As a corollary, we see, immediately, that in making such deposition rate calculations larger errors can be tolerated in ϵ than in the Lennard-Jones size parameter, σ)

8.3. Homologous Compounds: Reduction to the Univariate Case. In contrast, suppose we were dealing with an extensive family of heavy, straight-chain alkanes,⁸⁴ for which, say, $\sigma(m) \sim m^{0.51}$ and⁸³ $\epsilon(m) \sim m^{0.48}$. In that "degenerate" case $\dot{m}''(\mathbf{x}, t)$ would be approximately proportional to the i th moment of n with respect to m , written M_i , where $i \approx 0.29$. An interesting corollary of this fact is that the total mass deposition rate will not be very different from that calculated on the basis of the *mean* molecular weight of the alkane population. For example, if the alkane MMW was 282.55 (corresponding, say, to $n\text{-C}_{20}\text{H}_{42}$) and the spread (of a γ distribution) was, say, 100 amu, then the actual deposition rate would be only 1.3% less than an estimate based on the above-mentioned MMW!

It should be remarked that, in our discussion of each of the above limiting cases, we assumed, for simplicity, that $m \gg m(\text{N}_2)$ and $\sigma \gg \sigma(\text{N}_2)$, where N₂ is the background (carrier) gas. When such inequalities are not quite satisfied (i.e., if some of the suspended hydrocarbon species are "too light" or "too small"), then correction terms are clearly necessary, but QMOM techniques (section 5) could readily estimate $\dot{m}''(\mathbf{x}, t)$ via a Gaussian quadrature approximation to eq 4, with the full (nonpower law) expression for D_{eff} (ideal gas mixture) being used. Indeed, even the $D_{\text{eff}}^{2/3}$ approximation (often³³ valid for $Sc \gg 1$) can be relaxed⁸⁵ and the Ludwig–Soret contribution to the total deposition rate systematically included.⁸⁷

8.4. Coexisting Populations. Frequently we encounter intermediate situations in which there *coexist* a small, discrete number of homologous series ("families") of compounds, as in the case of, say, a mixture of both straight-chain and planar "ring" (say, PAH) compounds. In such cases, the above-mentioned state variables m , σ , ϵ , δ , α , and ω will again be "correlated", this time falling into possibly overlapping "bands" or "ensembles" in this hyperspace of state variables. Such problems can best be treated by introducing a continuous description for *each of the coexisting populations*,

i.e., one pdf for the straight chains, one for the ring compounds, etc. Each of these populations would then be tracked via its moments, etc. This is analogous to the common situation in aerosol dynamics in which one deals with a multimodal (mixed-origin or "history") population.⁷¹ While not exploiting moment methods, an interesting recent CMT example involving three coexisting populations (three "indices") is given in ref 88.

8.5. Combining Rules and Parameter Estimation. Indeed, there are many instructive parallels between the continuous (molecular) mixture theory and the *aerosol population balance* theory. We have to deal with systematic departures from arithmetic mean diameter "combining rules", which are not only important for the encounters of fractal aggregates²⁴ but also important at the *molecular level* [e.g., for nonspherical straight-chain alkane-alkane Lennard-Jones intermolecular size parameters (see, e.g., refs 33 and 89)]. From this viewpoint, the FA-FA' collision (coagulation rate constant) problem²⁴ shares many features with the problem of predicting σ_{ij} for the orientation-averaged interactions of, say, large, highly "branched" alkane molecules in fluid (vapor, liquid) mixtures.

8.6. Summary: Multivariate PBE Approach to CMT. We conclude this brief excursion into CMT with the overall statement that the population balance methods/approaches emphasized in this paper for bona fide nonspherical particle suspensions (aerosols and hydrosols) carry over to continuous (*molecular*) mixtures, which are particularly prevalent in petroleum⁹⁰ and combustion-engineering^{91,92} applications. Specific applications of QMOM to *nonequilibrium* CMT (e.g., the vaporization⁹² or combustion⁹³ of a multicomponent liquid fuel droplet), beyond the scope of this paper, will be presented separately.^{87,93}

9. Concluding Remarks

Generalizing our earlier work on univariate suspended particle populations (cast in terms of particle *volume* alone), we argue that most current/future population balance problems of SRE interest will require a *multivariate* description for the state of each particle. The recent experience we have gained with one rather effective bivariate model (based on particle *volume* and wetted *surface area*) has been reviewed here not only because many of its consequences are of immediate engineering utility but also because the multivariate strategy and computational methods we have developed/used for this particular bivariate case are expected to be of more general applicability.

The two computational methods emphasized/illustrated here are rather different from one another. One is explicitly stochastic (probabilistic) in nature and bears the name MC (section 5) because it invokes a random number generator in the course of simulating the collision term in the so-called PBE. As the required number of state variables grows beyond the two explicitly considered here, this class of MC methods seems likely to assume even greater importance.

In contrast to an early pessimistic assessment,⁹⁴ we have found that a bivariate *moment method* is not only possible but also rather effective for SRE simulation purposes!^{12,26} Indeed, the bivariate quadrature version of MOM discussed here (section 5) not only is able with only nine moments to capture the essential features of the overall moment surface (Figure 2) but also lends itself to dynamical simulations far from the asymptotic condition of near bivariate self-preservation. Also, un-

doubtedly most important, because the coupled moment equations are of the convection-diffusion-source (PDE) form, they can be readily incorporated in existing/future CFD simulation schemes.

Irrespective of the method by which they have been computed, or whether the values are evolving in space or time, we have shown that certain dimensionless mixed moments of the jpdf of particle *volume* and *surface area* are of special practical/statistical significance, as in the case of mass transfer to/from such coagulating + sintering aerosol populations. This includes (Table 1) (a) diffusion-controlled aerosol mass deposition across laminar forced-convection boundary layers and (b) the scavenging power of such suspended aerosols for vapors present in the carrier gas. Numerical estimates of these particular asymptotic mixed moments have recently been provided for both important Knudsen number limits (free molecule and continuum) and for arbitrary ratios of the characteristic time for Brownian *coagulation* to the characteristic time for sintering (*fusion*). Moreover, we have shown that this general approach, for any self-consistent combination of $Dam_f \equiv t_{coag}/t_f$ and fractal dimension, D_f , provides rational, systematic correction factors to preliminary engineering estimates based only on *mean* properties (here number-mean particle *volume* ϕ/N_p and number-mean particle *area* a'''/N_p) of the suspended particle population (see appendix 1). This approach can be extended to other population properties of interest, including those associated with the interaction of such aerosols with electromagnetic radiation, as in laser probing.^{10,95,96} Of course, often, the observables of interest *cannot* be simply expressed in terms of a small number of particular mixed moments but must be reconstructed by numerical quadratures over the corresponding jpdf(v, a) (see, e.g., ref 12 for the prediction of LLS; for a recent univariate example, see ref 30).

In section 8 we point out that the multistate variable population balance methods/approaches emphasized in this paper for bona fide nonspherical *particle* suspensions (aerosols and hydrosols), also carry over to so-called "(semi-)continuous (macro-)molecular mixtures". Indeed, we now anticipate rapid advances in nonequilibrium CMT, making use of several of the techniques emphasized in this overview.

In summary, the methods described here (section 5) for computing the underlying jpdf, or a selected subset of its mixed moments, should open the door to practical predictive methods for the dynamical evolution (in time and/or 3D physical space) of both multivariate *particle* and/or *molecule* populations, including cases (e.g., the atmosphere, combustors, particle synthesis reactors, etc.) where such multivariate populations inevitably interact with one another and the initially unmixed flows are "turbulent".

Acknowledgments

This interdisciplinary paper, emphasizing both MC- and moment-based methods to describe the evolution of multivariate particle populations, is dedicated to Prof. (Emeritus) Octave Levenspiel. His remarkable record of talks, papers, and books, many dealing with multiphase chemical reaction engineering, have stimulated us all and continue to motivate important new research. It is also a pleasure to acknowledge the financial support of NSF [Grants CTS-987 1885 and 998 0747 (Yale) and NASA Interagency Agreement W-18,429 (BNL)] and helpful discussions/correspondence with D.

L. Wright, Y. Xing, U. O. Koçlu, L. R. Collins, R. O. Fox, D. L. Marchisio, R. B. Diemer Jr., J. Fernandez de la Mora, A. Firoozabadi, A. V. Filippov, S. K. Friedlander, J. L. Castillo, P. Garcia-Ybarra, M. Arias-Zugasti, I. M. Kennedy, B. La Mantia, A. G. Konstandopoulos, C. M. Sorensen, J. J. Pyykonen, S. Rogak, and M. Zurita-Gotor. This overview of our recent multivariate population balance research has its roots in a paper [session: T1d08-Extended Abstract. *Proceedings of the Fourth International Particle Technology Forum* (CD-ROM available via AICHE)]²⁵ originally presented at the AICHE 2000 Annual Meeting, Los Angeles, CA, Nov 2000.

Appendix 1. Significance of Dimensionless Mixed Moments for Power-Law Kernels (Weighting Functions)

We explicitly demonstrate in the following that, for power-law kernels, the dimensionless mixed moments quantify the error associated with “crudely” assuming that all particles have the mean values of the relevant state variables. As a generic example, consider that the relevant state variables are particle *volume* and *surface area*, and we are interested in a quantity (particle “property”) adequately described by a power-law kernel of the form

$$k(v, a) = G \cdot v^k a^l \quad (\text{A1.1})$$

where G is some environment-dependent constant. For a normalized distribution $f(v, a) = n/N_p$, the “true” result will take the form

$$R_1 = N_p G \int \int v^k a^l f(v, a) dv da = G M_{k,l} \quad (\text{A1.2a})$$

where the integrations are from 0 to ∞ and $N_p = M_{0,0}$ is the total number of particles per unit volume. The crude assumption that all particles have the *mean* values of the relevant state variables, on the other hand, gives

$$R_0 = N_p \cdot G \cdot (\bar{v})^k (\bar{a})^l \quad (\text{A1.2b})$$

with $\bar{v} = M_{1,0}/M_{0,0}$ and $\bar{a} = M_{0,1}/M_{0,0}$. Defining the *dimensionless* mixed moment

$$\mu_{k,l} = \left(\frac{M_{k,l}}{M_{0,0}} \right) \left(\frac{M_{0,0}}{M_{1,0}} \right)^k \left(\frac{M_{0,0}}{M_{0,1}} \right)^l \quad (\text{A1.3})$$

and combining with eqs A1.2 yield the correction factor (ratio)

$$R \equiv R_1/R_0 = \mu_{k,l} \quad (\text{A1.4})$$

i.e., the above-mentioned “reference rate” must be multiplied by the correction factor $\mu_{k,l}$ to obtain the correct result. For a distribution that is “monodisperse” in each of the relevant state variables, the mixed moment and correction factor are, of course, unity. Equation A1.4 is a general result that does not assume any conditions on the jpdf, other than the existence of its moments. However, again, the kernel of interest must be of the power-law form. Applications of this result for the particular univariate case of *mass deposition from suspensions* to solid surfaces (immersed or containment) were given in refs 27 and 28. For the bivariate case (v, a), see section 3, Table 1, and ref 25.

Because the dimensionless mixed moments are surrogates for the local jpdf shape factors and are constants for a distribution that is self-preserving in the relevant mixed moments, for a self-preserving distribution the above-mentioned correction factors are constant. Note, also, that the *dimensionless* moments satisfy the same convexity relations (appendix 2) as the original moments, e.g.,

$$\frac{1}{\mu_{k,l}} \frac{\partial^2 \mu_{k,l}}{\partial k^2} = \frac{1}{M_{k,l}} \frac{\partial^2 M_{k,l}}{\partial k^2} \quad (\text{A1.5})$$

(see, e.g., Figure 2, which shows the surface $\mu(k, l)$ in the interval $0 \leq k \leq 3/2$; $0 \leq l \leq 3/2$).

Appendix 2. Proof of Mixed Moment Convexity

It is possible to show that $\log \mu_{k,l,\dots,m}$ is convex in each of its indices. This is equivalent to showing, for each moment index, the inequality

$$\frac{\partial^2 \log \mu_{k,l,\dots,m}}{\partial k^2} \geq 0 \quad (\text{A2.1})$$

where the indicated second derivative is taken by keeping the other indices l, \dots, m constant. In a particular bivariate case, with k being the volume exponent and l the surface area exponent, such a *concave upward* dimensionless moment surface is shown in Figure 2.

For a general proof, use the definition

$$\mu_{k,l,\dots,m} = \int \dots \int r^k s^l \dots t^m f(r, s, \dots, t) dr ds \dots dt \quad (\text{A2.2})$$

where each integration is over the entire positive range of state variables r, s, \dots from 0 to ∞ . We now carry out the differentiations (with the aid of $dr^k/dk = \log(r) r^k$) to obtain

$$\frac{\partial^2 \log \mu_{k,l,\dots,m}}{\partial k^2} = \frac{1}{\mu_{k,l,\dots,m}} \int \dots \int \log(r)^2 r^k s^l \dots t^m f(r, s, \dots, t) dr ds \dots dt$$

and

$$\begin{aligned} \frac{\partial^2 \log \mu_{k,l,\dots,m}}{\partial k^2} = & \frac{1}{\mu_{k,l,\dots,m}} \int \dots \int [\log(r)]^2 r^k s^l \dots t^m f(r, s, \dots, t) dr ds \dots dt - \\ & \frac{1}{\mu_{k,l,\dots,m}^2} \left[\int \dots \int \log(r) r^k s^l \dots t^m f(r, s, \dots, t) dr ds \dots dt \right]^2 \end{aligned} \quad (\text{A2.3})$$

It is convenient to define the (normalized) marginal distribution function

$$p(r) = \frac{1}{\mu_{k,l,\dots,m}} r^k \int \dots \int s^l \dots t^m f(r, s, \dots, t) ds \dots dt$$

in terms of which eq A2.3 becomes

$$\begin{aligned} \frac{\partial^2 \log \mu_{k,l,\dots,m}}{\partial k^2} = & \int [\log(r)]^2 p(r) dr - \left[\int [\log(r)] p(r) dr \right]^2 \geq 0 \end{aligned}$$

which completes the proof of eq A2.1. The inequality follows as a special case (with $\varphi(r) = 1$) of the Schwartz inequality with weight function $p(r)$:

$$[\int \psi(r) \varphi(r) p(r) dr]^2 \leq \int [\psi(r)]^2 p(r) dr \int [\varphi(r)]^2 p(r) dr \quad (\text{A2.4})$$

and similarly for the index l .

For a simple illustration of moment surface convexity in one dimension, consider the log-normal pdf: $f_{LN}(r, m, s) = (r\sqrt{2\pi})^{-1} \exp[-(\ln r - \ln m)^2/2s^2]$, where r is the ratio of the particle radius to the unit of length (e.g., 1 nm), m is the logarithm of the ratio of the count mean radius (i.e., geometric mean radius) to the unit of length, and s is the logarithm of the geometric standard deviation. The moments of $f_{LN}(r)$ are $M_{k,m,s} = \exp[km + (ks)^2/2]$, showing that $\log(M_k)$ is an upwardly curved parabolic function of k . An illustrative *multivariate* surface results upon consideration of the *factorable* (uncorrelated) log-normal distribution: $f(r_1, r_2, \dots) = f_{LN}(r_1, m_1, s_1) f_{LN}(r_2, m_2, s_2) \times \dots$. In this special case, the mixed moments are also factorable: $M_{k,l,\dots} = M_{k,m_1,s_1} M_{l,m_2,s_2} \times \dots$ and the corresponding moment surface (cf. Figure 2, with a non-logarithmic ordinate) is simply a multivariate quadratic form.

For the MOM closure scheme based on moment interpolation,³⁵ convexity is a helpful, if not essential, property. The QMOM technique (section 5)^{12,26,31,32} achieves closure without the need for moment interpolation or extrapolation.

Acronyms/Abbreviations

amu = atomic mass unit
 ASD = aggregate size distribution
 BC = black carbon
 BV = bivariate (two particle "state variables")
 CFD = computational fluid dynamics
 CMT = continuous mixture theory
 CPU = central processor unit (computer)
 1D = one-dimensional (univariate)
 Dam_f = Damkohler number for coalescence (fusion), t_{coag}/t_f
 DSMC = direct simulation Monte Carlo (for the Boltzmann equation)
 FA = fractal aggregate
 fct = function
 HTCRe = High-Temperature Chemical Reaction Engineering Laboratory
 IPDE = integro-partial differential equation
 jpdf = joint probability density function
 Kn = Knudsen number (gas mean free path/(2R_{mob}))
 LLS = laser light scattering
 LN = log-normal
 MC = Monte Carlo
 MOM = method of moments
 MMW = mean molecular weight
 MWD = molecular weight distribution
 MV = multivariate
 PAH = polycyclic aromatic hydrocarbon
 PBE = population balance equation
 PCA = principal component analysis
 PDE = partial differential equation
 pdf = probability density function
 Q = quadrature
 QMOM = quadrature method of moments
 RHS = right-hand side (of the equation)
 rms = root mean square

Sc = Schmidt number (for particle diffusion in a carrier fluid; ν/D_p)

SRE = sol reaction engineering

TEM = transmission electron microscope

TPS = thermophoretic sampling

Literature Cited

- Helble, J. J. Combustion Aerosol Synthesis of Nano-scale Ceramic Powders. *J. Aerosol Sci.* **1998**, 29 (5 and 6), 721–736.
- Pratsinis, S. E. Flame Aerosol Synthesis of Ceramic Powders. *Prog. Energy Combust. Sci.* **1998**, 24, 197–219.
- Wooldridge, M. S. Gas-Phase Combustion Synthesis of Particles. *Prog. Energy Combust. Sci.* **1998**, 24, 63–87.
- Friedlander, S. K. *Smoke Dust and Haze*; Oxford University Press: Oxford, U.K., 2000.
- Randolph, A. D.; Larson, M. A. *Theory of Particulate Processes*, 2nd ed.; Academic Press: New York, 1988. See also: Gerstlauer, A.; Mitrovic, A.; Motz, S.; Gilles, E.-D. A Population Model for Crystallization Processes Using Two Independent Particle Properties. *Chem. Eng. Sci.* **2001**, 56, 2553–2565.
- Randolph, T. W.; Randolph, A. D.; Mebes, M.; Yeung, S. Sub-micrometer-Sized Biodegradable Particles of Poly(L-Lactic Acid) via the Gas Antisolvent Spray Precipitation Process. *Biotechnol. Prog.* **1993**, 9, 429–435. See also: Yeo, S.-D.; Lim, G.-B.; Debenetti, P. G.; Bernstein, H. Formation of Microparticulate Protein Powders Using a Supercritical Fluid Antisolvent. *Biotechnol. Bioeng.* **1993**, 41, 341–346.
- Koch, W.; Friedlander, S. K. The Effect of Particle Coalescence on the Surface Area of a Coagulating Aerosol. *J. Colloid Interface Sci.* **1990**, 140, 419–427.
- Xing, Y.; Koylu, U. O.; Rosner, D. E. Synthesis and Restructuring of Inorganic Nano-particles in Counterflow Diffusion Flames. *Combust. Flame* **1996**, 107, 85–102.
- Xing, Y.; Koylu, U. O.; Rosner, D. E.; Tandon, P. Morphological Evolution of Nano-Particles in Laminar Counterflow Diffusion Flames—Measuring and Modeling. *AIChE J.* **1997**, 43(11A), 2641–2649.
- Xing, Y.; Koylu, U. O.; Rosner, D. E. In situ Light-Scattering Measurements of Morphologically Evolving Flame-Synthesized Oxide Nano-Aggregates. *Appl. Opt.* **1999**, 38 (12), 2686–2697 (Apr 20, 1999).
- Rosner, D. E.; Pyykonen, J. J.; McGraw, R. L.; Wright, D. L. Bivariate Moment Method Simulation of a Population of Coagulating and Sintering Alumina Nano-particles in a Laminar Diffusion Flame. AAAR2000, St. Louis, MO, Nov 2000.
- Rosner, D. E.; Pyykonen, J. J. Bivariate Moment Simulation of Coagulating and Sintering Nanoparticles in Flames. *AIChE J.* **2002**, 4 (3), 476–491.
- It has been suggested that China's increased severity of dust storms, commonly attributed to overfarming and deforestation, may be due to suspended black carbon.¹⁴
- Menon, S.; Hansen, J.; Nazarenko, L.; Luo, Y. Climate effects of black carbon aerosols in China and India. *Science* **2002**, 297, 2250–2253.
- Jacobson, M. Z. Analysis of Aerosol Interactions With Numerical Techniques for Solving Coagulation, Nucleation, Condensation, Dissolution and Reversible Chemistry Among Multiple Size Distributions. *J. Geophys. Res.* **2002**, 107 (D19), 4366 (DOI: 10.1029/2001).
- Tandon, P.; Rosner, D. E. Monte Carlo Simulation of Particle Aggregation and Simultaneous Restructuring. *J. Colloid Interface Sci.* **1999**, 213 (2), 273–286. See also: *Ind. Eng. Chem. Res.* **1995**, 34, 3265–3277.
- Rosner, D. E.; Yu, S. Monte Carlo Simulation of Aerosol Aggregation and Simultaneous Spheroidization. *AIChE J.* **2001**, 47 (3), 545–561.
- Tsantilis, S.; Pratsinis, S. E. Evolution of Primary and Aggregate Particle Size Distributions by Coagulation and Sintering. *AIChE J.* **2000**, 46 (2), 407–415.
- Tsantilis, S.; Kammler, H. K.; Pratsinis, S. E. Population Balance Modeling of Flame Synthesis of Titania Nano-particles. *Chem. Eng. Sci.* **2002**, 57, 2139–2156.
- Using direct off-lattice simulations, Fry et al. (Enhanced Kinetics and Free-Volume Universality in Dense Aggregating Systems. *Phys. Rev. Lett.* **2002**, 89 (14), 148301–1–4) have shown that if one introduces free- (and excluded-) volume corrections, then mean-field-predicted coagulation rates remain accurate up to the "gelation" threshold.

- (21) However, keep in mind that, in the absence of so-called "back-mixing", t could be a "Lagrangian" variable, i.e., elapsed time while following the motion of a "parcel" of suspension. This proved to be possible in the case of our steady laminar flames because size- and morphology-insensitive *thermophoresis* (Rosner et al. *Ind. Eng. Chem. Res.* **1992**, 31, 760–769) dominated Brownian diffusion (see, e.g., refs 11, 12, and 22 and Filippov, A. V.; et al. *J. Colloid Interface Sci.* **2000**, 229, 261).
- (22) Tandon, P.; Rosner, D. E. Sintering Kinetics and Transport Property Evolution of Large Multi-particle Aggregates. *Chem. Eng. Commun.* **1996**, 151, 147–168.
- (23) Xing, Y.; Rosner, D. E. Prediction of Spherule Size in Gas-Phase Nano-Particle Synthesis. Special Issue on Vapor Phase Synthesis. *J. Nanopart. Res.* **1999**, 1, 277–291.
- (24) Zurita-Gotor, M.; Rosner, D. E. Effective Diameters for Collisions of Fractal-like Aggregates: Recommendations for Improved Aerosol Coagulation Frequency Predictions. *J. Colloid Interface Sci.* **2002**, 255, 10–26.
- (25) Rosner, D. E.; Tandon, P.; McGraw, R. L.; Wright, D. L. Relevant "Mixed" Moments for the Calculation of Deposition, Vapor Scavenging, and Optical Properties of Populations of Nonspherical Suspended Particles. *Proceedings of the Fourth Particle Technology Forum*; AIChE: New York, 2000 (session T1d08; available as CD-ROM).
- (26) Wright, D. L.; McGraw, R.; Rosner, D. E. Bi-variate Extension of the Quadrature Method of Moments for Modeling Simultaneous Coagulation and Particle Sintering. *J. Colloid Interface Sci.* **2001**, 236, 242–251.
- (27) Rosner, D. E. Total Mass Deposition Rates from Polydispersed Aerosols. *AIChE J.* **1989**, 35 (1), 164–167.
- (28) Rosner, D. E.; Tassopoulos, M. Deposition Rates from "Polydispersed" Particle Populations of Arbitrary Spread. *AIChE J.* **1989**, 35 (9), 1497–1508. See also: *J. Aerosol Sci.* **1991**, 22 (7), 843–867.
- (29) Rosner, D. E.; Khalil, Y. F. Morphology Effects on Polydispersed Aerosol Deposition Rates. *Trans. Am. Nucl. Soc.* **1997**, 77 (TANSO 77-1-560), 425–427.
- (30) Rosner, D. E.; Khalil, Y. F. Particle Morphology- and Knudsen Transition Effects on Thermophoretically Dominated Total Mass Deposition Rates From "Coagulation-Aged" Aerosol Populations. *J. Aerosol Sci.* **2000**, 31 (3), 273–292.
- (31) McGraw, R. Description of Aerosol Dynamics by the Quadrature Method of Moments. *Aerosol Sci. Technol.* **1997**, 27, 255–265.
- (32) Marchisio, D. L.; Pikturna, J. T.; Fox, R. O.; Vigil, D. R. Quadrature Method of Moments for Population Balances with Nucleation, Growth and Aggregation. *AIChE J.* **2003**, 49, in press.
- (33) Rosner, D. E. *Transport Processes in Chemically Reacting Flow Systems*; Dover: New York, 2000.
- (34) A prospect not explicitly addressed by Frenklach.^{35,36}
- (35) Frenklach, M.; Harris, S. J. Aerosol Dynamics Modeling Using the Method of Moments. *J. Colloid Interface Sci.* **1987**, 118, 252–261.
- (36) Frenklach, M. Method of Moments with Interpolative Closure. *Chem. Eng. Sci.* **2002**, 57, 2229–2239.
- (37) Wright, D. L.; McGraw, R.; Benkovitz, C. M.; Schwartz, S. E. Six-moment Representation of Multiple Aerosol Populations in a Sub-hemispheric Chemical Transport Model. *Geophys. Res. Lett.* **2000**, 7, 967. See also: Tatang, M. A.; et al. An Efficient Method for Parametric Uncertainty Analysis of Numerical Geophysical Models. *J. Geophys. Res.* **1997**, 102 (D18), 21925–21932.
- (38) Yoon, C.; McGraw, R. Multivariate Extension of the Quadrature Method of Moments for Modeling Generally-mixed Particle Populations. 2003, in preparation.
- (39) Wright, D. L. Retrieval of Optical Properties of Atmospheric Aerosols from Moments of the Particle Size Distribution. *J. Aerosol Sci.* **2000**, 31 (1), 1–18.
- (40) Rosner, D. E.; Garcia-Ybarra, P.; Mackowski, D. W. Size and Structure-Insensitivity of the Thermophoretic Transport of Aggregated "Soot" Particles in Gases. *Combust. Sci. Technol.* **1991**, 80, 87–101.
- (41) Rosner, D. E.; Zurita, M.; Filippov, A. V.; Fernandez de la Mora, J. Orientation-averaged Free-molecule Drag Correlation for Nonspherical Particles Described by Their Volume and Surface Area. AIChE Meeting, Los Angeles, CA, Nov 2000.
- (42) Fernandez de la Mora, J. Free-Molecular Mobility of Polyhedra and Other Convex Hard Bodies. *J. Aerosol Sci.* **2002**, 33, 477–489.
- (43) Willman, B. T.; Teja, A. S. Continuous Thermodynamics of Phase Equilibria Using a Multi-variate Function and an Equation of State. *AIChE J.* **1986**, 32 (12), 2067–2078.
- (44) In a recent analysis of the transitional heat flux in a gas-filled nonisothermal gap, using a linearized Boltzmann equation for the case of a Maxwellian monatomic gas, Struchtrup⁴⁵ has employed up to 48 one-dimensional moment equations (first-order ODEs) to obtain converged results. Computational times for a given Knudsen number are, however, smaller than those if the DSMC method were used (see also: Rosner, D. E.; Papadopoulos, D. H. Jump, Slip and Creep Boundary Conditions at Nonequilibrium Gas/Solid Interfaces. *Ind. Eng. Chem. Res.* **1995**, 35 (9), 3210–3222).
- (45) Struchtrup, H. Heat Transfer in the Transition Regime: Solution of Boundary Value Problems for Grad's Moment Equations via Kinetic Schemes. *Phys. Rev. E* **2002**, 65, 41204.
- (46) Spielman, L. A.; Levenspiel, O. A Monte-Carlo Treatment for Reacting and Coalescing Dispersed Phase Systems. *Chem. Eng. Sci.* **1965**, 20, 247–254.
- (47) Shah, B. H.; Borwanker, J. D.; Ramakrishna, D. Simulation of Particulate Systems Using the Concept of the Interval of Quiescence. *AIChE J.* **1977**, 23, 897. See also: *Chem. Eng. Sci.* **1977**, 32, 1419.
- (48) Ramakrishna, D. Analysis of Population Balance—IV. The Precise Connection Between Monte Carlo Simulation and Population Balances. *Chem. Eng. Sci.* **1981**, 36, 1203.
- (49) Wu, M. K.; Friedlander, S. K. Enhanced Power Law Agglomerate Growth in the Free-Molecular Regime. *J. Aerosol Sci.* **1993**, 24 (3), 273.
- (50) Smith, M.; Matsoukas, T. Constant Number Monte-Carlo Simulation of Population Balances. *Chem. Eng. Sci.* **1997**, 53 (9), 1777–1786.
- (51) Ramakrishna, D. *Population Balances—Applications to Particulate Systems in Engineering*; Academic Press: Orlando, FL, 2000; *Chem. Eng. Sci.* **2002**, 57, 595–606. See also: Diemer, R. B. Moment Methods for Coagulation, Breakage, and Coalescence Problems. Ph.D. Dissertation, Chemical Engineering Department, University of Delaware, 1999. Diemer, R. B.; Olson, J. H. A Moment Methodology for Coagulation and Breakage Problems: Part 1—Analytical Solution of the Steady-State Population Balance. *Chem. Eng. Sci.* **2002**, 57, 2193–2209. Diemer, R. B.; Olson, J. H. A Moment Methodology for Coagulation and Breakage Problems: Part 2—Moment Models and Distribution Reconstruction. *Chem. Eng. Sci.* **2002**, 57, 2211–2228.
- (52) Gooch, J. R. P.; Hounslow, M. J. Monte Carlo Simulation of Size-Enlargement Mechanisms in Crystallization. *AIChE J.* **1996**, 42 (7), 1864–1874.
- (53) Bird, G. A. *Molecular Gas Dynamics and the Direct Simulation of Gas Flows*; Clarendon Press: Oxford, U.K., 1994.
- (54) Efendiev, Y.; Zachariah, M. R. Hybrid Monte-Carlo Method for Simulation of Two Component Aerosol Coagulation and Phase Segregation. *J. Colloid Interface Sci.* **2002**, 249 (1), 30–43.
- (55) Kostoglu, M.; Konstantopoulos, A. G. Brownian Coagulation of Fractal Aggregates. *J. Aerosol Sci.* **2000**, 31, S574 (Supplement 1).
- (56) Laurenzi, I. J.; Bartels, J. D.; Diamond, S. L. A General Algorithm for Exact Simulation of Multicomponent Aggregation Processes. *J. Comput. Phys.* **2002**, 177, 418–449.
- (57) Gillespie, D. T. An Exact Method for Numerically Simulating the Stochastic Coalescence Process in a Cloud. *J. Atmos. Sci.* **1975**, 32, 1977.
- (58) Fichtorn, K. A.; Weinberg, W. H. Theoretical Foundation of Dynamical Monte Carlo Simulations. *J. Chem. Phys.* **1991**, 95 (2), 1090–1096.
- (59) Lin, Y.; Lee, K.; Matsoukas, T. Solution of Population Balance Equation Using Constant-Number Monte Carlo. *Chem. Eng. Sci.* **2002**, 57 (12), 2241–2252.
- (60) Eibeck, A.; Wagner, W. An Efficient Stochastic Algorithm for Studying Coagulation Dynamics and Gelation Phenomena. *SIAM J. Sci. Comput.* **2000**, 22 (3), 802.
- (61) Goodson, M.; Kraft, M. An Efficient Stochastic Algorithm for Simulating Nano-Particle Dynamics. *J. Comput. Phys.* **2002**, 183, 210–232.
- (62) Manjunath, S.; Gandhi, K. S.; Kumar, R.; Ramakrishna, D. Precipitation in Small Systems—I. Stochastic Analysis. *Chem. Eng. Sci.* **1994**, 49, 1451–1463. See also: Manjunath, S.; Gandhi, K. S.; Kumar, R.; Ramakrishna, D. Precipitation in Small Systems—Part II. Mean Field Equations More Effective Than Population Balance. *Chem. Eng. Sci.* **1996**, 51, 4423–4436.

- (63) Zurita-Gotor, M.; Rosner, D. E. Aggregate Size Distributions Resulting From Brownian Coagulation in the Free-Molecule Limit; Sensitivity to an Improvement in the FA Coagulation Rate Constant. AAAR Meeting, Charlotte, NC, Oct 2002. *J. Colloid Int. Sci.* (submitted).
- (64) Kazakov, A.; Frenklach, M. Dynamic Modeling of Soot Particle Coagulation and Aggregation: Implementation with the Method of Moments and Application to High-Pressure Laminar Premixed Flames. *Combust. Flame* **1998**, *114*, 484–501.
- (65) Xiong, Y.; Pratsinis, S. E. Formation of Agglomerate Particles by Coagulation and Sintering—Part I. A Two-dimensional Solution of the Population Balance Equation. *J. Aerosol Sci.* **1993**, *24*, 283–300. See also: Xiong, Y.; Pratsinis, S. E. *J. Aerosol Sci.* **1993**, *24*, 301–313.
- (66) Gelbard, F.; Tambour, Y.; Seinfeld, J. H. Sectional Representations for Simulating Aerosol Dynamics. *J. Colloid Interface Sci.* **1980**, *76*, 541–556.
- (67) Jeong, J. I.; Choi, M. A Sectional Method for the Analysis of Growth of Polydisperse Non-Spherical Particles Undergoing Coagulation and Coalescence. *J. Aerosol Sci.* **2001**, *32*, 565–582.
- (68) Jacobson, M. Z. Strong Radiative Heating due to the Mixing State of Black Carbon in Atmospheric Aerosols. *Nature* **2001**, *409*, 695–697.
- (69) McGraw, R. M.; Wright, D. Chemically Resolved Aerosol Dynamics for Internal Mixtures by the Quadrature Method of Moments. *J. Aerosol Sci.* **2003**, *34*, 189–209.
- (70) However, instead of using a full sectionalization, the multivariate space is sampled using multiple one-dimensional distributions. For example, Jacobson uses 18 distributions, each with 60 size classes to sample a multivariate space of 30 species. The distributions interact through coagulation. The main issues are selection of the distributions and the large number of variables that need to be tracked (e.g., in Jacobson's calculation, this is 18 size distributions \times an average of 30 species per distribution \times 60 size bins per species per distribution = 32 400 concentrations in a single spatial grid cell).¹⁵
- (71) Whitby, E. R.; McMurry, P. H. Modal Aerosol Dynamics Modeling. *Aerosol Sci. Technol.* **1997**, *27* (6), 673–688 (Dec). See also: *J. Aerosol Sci.* **2000**, *33* (4), 623–645.
- (72) Wilck, M. Modal Modeling of Multicomponent Aerosols (Akademische Abhandlungen zu den Geowissenschaften). Ph.D. Dissertation, Leipzig University, Leipzig, Germany, 1999.
- (73) Some observables can be shown to be expressible in terms of "surprising" mixed moments; a good example is the average number of spherules per aggregate, written \bar{N} . Because $6\pi a$ plays the role of an effective spherule diameter in an aggregate of total volume v , one can show that N_{eff} can be expressed as $a^3/(36\pi v^2)$, revealing that \bar{N} can be expressed in terms of the particular moment $M_{-2,3}$.
- (74) These "assignments", beyond the scope of the present brief overview, are suggested/deferred in a full-length account of this QMOM modeling effort.¹²
- (75) Lehtinen, K. E. J.; Zachariah, M. R. Energy Accumulation in Nano-particle Collision and Coalescence Processes. *J. Aerosol Sci.* **2002**, *33*, 357–368.
- (76) Gal-Or, B.; Cullinan, H. T., Jr.; Galli, R. New Thermodynamic Transport Theory for Systems with Continuous Component Density Distributions. *Chem. Eng. Sci.* **1975**, *30*, 1085–1092.
- (77) Cotterman, R. L.; Prausnitz, J. M. Flash Calculations For Continuous or Semi-Continuous Mixtures Using an Equation of State. *Ind. Eng. Chem. Process Des. Dev.* **1985**, *24* (2), 433–443.
- (78) Cotterman, R. L.; Chou, G. F.; Prausnitz, J. M. Comments on Flash Calculations For Continuous or Semi-Continuous Mixtures Using an Equation of State. *Ind. Eng. Chem. Process Des. Dev.* **1986**, *25* (3), 840–841.
- (79) Shibata, S. K.; Sandler, S. I.; Behrens, R. A. Phase Equilibrium Calculations For Continuous and Semi-Continuous Mixtures. *Chem. Eng. Sci.* **1987**, *42* (8), 1977–1988.
- (80) Kincaid, J. M.; de Haro, M. L.; Cohen, E. G. D. Irreversible Thermodynamics of Polydispersed Fluids. *Int. J. Thermophys.* **1988**, *9* (6), 1031–1040.
- (81) McCoy, B. J. Distribution Kinetics for Temperature-Programmed Pyrolysis. *Ind. Eng. Chem. Res.* **1999**, *38*, 4531–4537.
- (82) For substances with a common value of $Z_c (=p_c V_c/RT_c)$, the critical parameters $V_c^{1/3}$ [or even $(T_c/P_c)^{1/3}$] and T_c can be used as surrogates for (proportional to) σ and ϵ , respectively (see, e.g., ref 33).
- (83) Indeed, following Tee et al. *Ind. Eng. Chem. Fundam.* **1966**, *5*, 356–363, both σ and ϵ/k_B have been corrected (method ix) for nonzero ω . More generally, an engineering approach to the inclusion of the effects of nonzero α and δ is to also let them influence the "effective" values of σ and ϵ and the associated collision integral. See, e.g.: Brokaw, R. S. *Ind. Eng. Chem. Process Des. Dev.* **1969**, *8*, 240.
- (84) Rosner, D. E.; La Mantia, B.; Arias-Zugasti, M. Non-equilibrium Continuous Mixture Reformulation of the Canonical Isobaric Dew Point Problem, Including Soret Separation Effects. *AIChE J.* **2003**, submitted for publication.
- (85) For example, if the correction term to the $Sc^{-2/3}$ dependence of St_{lm} is of the form $1 - 0.2980Sc^{-1/3} + \dots$ (e.g., for laminar rotating disk flow⁸⁶), then one merely has to demonstrate that this correction factor, with Sc evaluated for the mean molecular weight "solute", is sufficiently close to unity.
- (86) Newman, J. *Electrochemical Systems*; Prentice Hall: Englewood Cliffs, NJ, 1991.
- (87) Rosner, D. E.; La Mantia, B.; Arias-Zugasti, M. Continuous Mixture Formulation of the Canonical Isobaric Dew-Point Problem, Including Soret Separation. *AIChE J.* **2003**, submitted for publication.
- (88) Piexoto, P. C.; Platt, G. M.; Pessoa, F. L. P. Vapor–Liquid Equilibria of Multi-Indexed Continuous Mixtures Using an Equation of State and Group Contribution Methods. *Chem. Eng. J.* **2000**, *77*, 179–187.
- (89) Pamies, J.; Vega, L. Vapor–Liquid Equilibria and Critical Behavior of Heavy *n*-Alkanes Using Transferable Parameters from the Soft-SAFT Equation of State. *Ind. Eng. Chem. Res.* **2001**, *40*, 2532–2543.
- (90) Firoozabadi, A. *Thermodynamics of Hydrocarbon Reservoirs*; McGraw-Hill: New York, 1999.
- (91) Hallett, W. L. H. A Simple Model for the Vaporization of Droplets With Large Numbers of Components. *Combust. Flame* **2000**, *121*, 334–344.
- (92) Zhu, G.-S.; Reitz, R. D. A Model for High-Pressure Vaporization of Droplets of Complex Liquid Mixtures Using Continuous Thermodynamics. *Int. J. Heat Mass Transfer* **2002**, *45*, 495–507.
- (93) Arias-Zugasti, M.; Rosner, D. E. Multi-component Fuel Droplet Vaporization and Combustion Using Spectral Continuous Mixture Theory. *Combust. Flame* **2003**, submitted for publication.
- (94) Hulburt, H. M.; Katz, S. Some Problems in Particle Technology—A Statistical Mechanics Formulation. *Chem. Eng. Sci.* **1966**, *17*, 555–574. See also: *Ind. Eng. Chem. Fundam.* **1969**, *8*, 319–324.
- (95) Sorensen, C. M. Scattering of Light by Fractal Aggregates: A Review. *Aerosol Sci. Technol.* **2001**, *35* (2), 640–648.
- (96) Sorensen, C. M.; Wang, G. M. Size Distribution Effect on the Power-Law Regime of the Structure Factor for Fractal Aggregates. *Phys. Rev. E* **1999**, *60*, 7143.

Note Added in Proof: Recently, methods have been developed for the *direct propagation of quadrature abscissas and weights*, circumventing many of the problems associated with repetitive moment inversion in computational models employing QMOM [see the Jacobian matrix transformation (JMT) method introduced in ref 69 and applied in ref 63, as well as the approaches of Marchisio, D. L.; Fox, R. O. Direct Quadrature Method of Moments: Derivation, Analysis and Applications. *J. Comput. Phys.* **2003**, in press and Fox, R. O. *Computational Models for Turbulent Reacting Flows*; Cambridge University Press: Cambridge, U.K., 2003; Appendix B]. Both of these "direct" approaches employ Jacobian matrices constructed from the set of equations defining the (one-to-one) correspondence between moments and quadrature abscissas ("nodes") and weights. Thus, in effect, Eulerian transport equations (PDEs) are derived for the multivariate abscissas (nodes) and weights, treated as "pseudosppecies".

Received for review August 8, 2002

Revised manuscript received February 28, 2003

Accepted March 3, 2003

IE020627L